International Journal of Mathematical Archive-7(4), 2016, 45-57
Available online through www.ijma.info ISSN 2229 – 5046

EFFECT OF HALL CURRENTS, THERMOPHORESIS ON THE MHD MIXED CONVECTIVE FLOW PAST A PERMEABLE STRETCHING SURFACE WITH THERMAL RADIATION

KALYANI Ch[1], SREELAKSHMI K[2] AND SAROJAMMA G[3,*]

[1, 2, 3] **Department of Applied Mathematics,**
Sri Padmavati Mahila Visvavidyalayam, Tirupati-517502, India.

(Received On: 04-04-16; Revised & Accepted On: 17-04-16)

ABSTRACT

The present analysis deals with the effect of Hall currents, thermal radiation on the mixed convection flow of a viscous incompressible electrically conducting fluid past an unsteady porous stretching sheet embedded in a porous medium under the influence of transverse uniform magnetic field in the presence of thermophoresis and chemical reaction with convective boundary condition. Numerical solutions of the governing equations are obtained using Keller-box technique. The profiles of primary and secondary velocities, temperature and concentration are graphically presented for various values of suction parameter, thermal radiation parameter, Hall parameter, magnetic parameter etc. The values of local skin friction coefficient, local Nusselt number and local Sherwood number are tabulated for various values of parameters that occur in the analysis.

Keywords: *MHD, Hall currents, convective boundary condition, thermophoresis.*

1. INTRODUCTION

Thermophoresis is a phenomenon in which micro-sized particles, when suspended in a gas with thermal gradient, experience a force which causes the small particles to move from a hot surface towards a colder one. The force experienced by these particles as a result of the temperature gradient is known as thermophoretic force and the velocity with which the particles move is called the thermophoretic velocity. Thermophoresis is found to be one of the important mechanisms of mass transfer in the process of modified chemical vapor deposition (MCVD). This phenomenon plays a significant role in a wide range of applications such as the production of ceramic powders in high temperature aerosol flow reactors and optical fibers obtained by the MCVD process. It is observed that the thermophoretic deposition of the radioactive particles to be one of the reasons for the occurrence of accidents in the nuclear reactors. The principle of thermophoresis is employed in the manufacturing of graded index silicon dioxide and germanium dioxide optical fiber. Goldsmith and May (1966) appear to be the first researchers to investigate the thermophoretic transport in a one-dimensional flow to measure the thermophoretic velocity. Hales *et al.* (1972) studied the thermophoretic deposition of the aerosol particles on to an isothermal vertical surface situated adjacent to a large body of an otherwise quiescent air- stream-aerosol mixture. Selim *et al.* (2003) studied the effects of thermophoresis and non uniform surface mass flux on the mixed convection flow past a heated vertical permeable plate.

The study of Hall currents is important as these currents have a significant effect on the magnitude and the direction of current density and thus on the magnetic force term. The effect of Hall currents on MHD free convective flow has several industrial applications such as in power generators, electric transformers, heating elements and MHD accelerators.The study of boundary layer flow and heat transfer of fluids over a continuous stretching surface attracted the attention of several researchers owing to its wide range of engineering and industrial applications, especially in the manufacturing of glass fiber, polymer sheets, plastic films and metal wires etc. It is reported that the quality of the final product in the polymer glass and plastic industry depends considerably on the rate of cooling. Sakiadis (1961) made the first investigation to understand the boundary layer flow over a continuous stretching surface. Following this study several researchers analyzed the boundary layer flow over stretching surface with different conditions. Vajravelu (1994) analysed the convective heat transfer and flow of a viscous fluid near a permeable stretching surface. Eldahab et al. (2007) studied effect of Hall current on the MHD convection flow from an inclined continuous permeable stretching surface in the presence of temperature dependent internal heat generation/absorption. Salem and Aziz (2008) analysed the effect of Hall current and chemical reaction on the steady flow, heat and mass transfer laminar of a viscous, electrically conducting fluid over a continuously stretching surface in the presence of heat generation/absorption. Aziz (2010) investigated the flow and heat transfer of a viscous fluid flow over an unsteady stretching surface with Hall effects. Dulal Pal (2013) studied the influence of Hall current and thermal radiation on flow and heat transfer characteristics in a viscous fluid over an unsteady stretching permeable surface.

Thermal radiation plays a vital role in manufacturing process in industry. For example, in casting and levitation, metallic rolling, design of furnace and fins etc. In engineering, many processes involve very high temperatures and the application of radiative heat transfer is essentially required to design the specific equipment. Nuclear power plants, gas turbines, satellites and space vehicles are some of the examples (Seddeek (2002)) which involve radiative heat transfer.

In this paper we made an effort to study the effects of Hall currents, thermophoresis and heat source/sink on the unsteady flow of a viscous incompressible electrically conducting fluid past a porous stretching sheet embedded in a porous medium subject to a transverse magnetic field in the presence of first order chemical reaction with velocity slip and convective heat boundary conditions.

2. MATHEMATICAL FORMULATION

Consider the unsteady flow, heat and mass transfer of a viscous, incompressible and electrically conducting fluid past a vertical permeable stretching sheet coinciding with the plane $y = 0$ and the flow is confined to the region $y > 0$. A schematic representation of the physical model is shown in Fig. 1.

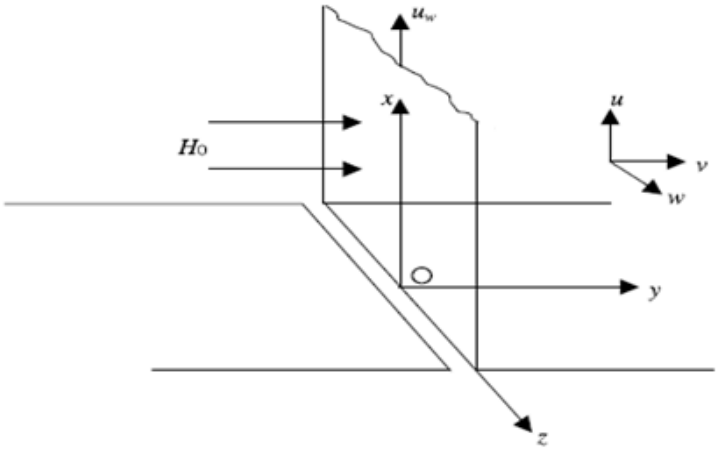

Fig. 1: Physical model and coordinate system

We choose the frame of reference (x, y, z) such that the x-axis is along the direction of motion of the surface, the y-axis is normal to the surface and the z-axis transverse to the xy-plane. An external constant magnetic field H_0 is applied in the positive y-direction. The effects of thermophoresis, thermal radiation and chemical reaction are considered.

Taking Hall effects into consideration and assuming that the electron pressure gradient, the ion slip and the thermo-electric effects are negligible, the generalized Ohm's law can be written as (Sutton and Sherman (1965))

$$\boldsymbol{j} = \sigma\left[\boldsymbol{E} + \mu_e \boldsymbol{q} \times \boldsymbol{H} - \frac{\mu_e}{e n_e}\boldsymbol{j} \times \boldsymbol{H}\right] \quad (1)$$

where n_e and e stand for the electron number density and the electric charge, respectively, $\sigma(\sigma = \frac{e^2 n_e T_e}{m_e})$ is the electrical conductivity, T_e and m_e denote the electron collision time and the mass of an electron respectively. The effect of Hall current gives rise to a force in the z-direction resulting in a cross-flow in this direction and thus the flow becomes three-dimensional. where (u, v, w), (E_x, E_y, E_z) and (j_x, j_y, j_z) are the components of $\boldsymbol{q}$, $\boldsymbol{E}$ and $\boldsymbol{j}$ respectively. In this study, we assume that the magnetic Reynolds number is small $(Re_m \ll 1)$ so that the induced magnetic field is negligible. j_y is a constant due to the equation of conservation of electric charge $\nabla.\boldsymbol{j} = 0$. Since $j_y = 0$ at the plate which is electrically non-conducting, we obtain $j_y = 0$ everywhere in the flow.

Hence (1) reduces to

$$J_x = \frac{\sigma B}{(1+m^2)}(mu - w) \quad (2)$$

$$J_z = \frac{\sigma B}{(1+m^2)}(u + mw) \quad (3)$$

where (u, v, w) are the velocity components in the (x, y, z) directions respectively, m $(= \omega_e t_e)$ is the Hall parameter, $B = \mu_e H_0$ is the strength of the imposed magnetic field and ω_e is the electron frequency.

The continuity, momentum, energy and concentration equations governing such type of flow can be written as

$$\frac{\partial u}{\partial x} + \frac{\partial v}{\partial y} = 0 \quad (4)$$

$$\frac{\partial u}{\partial t} + u\frac{\partial u}{\partial x} + v\frac{\partial u}{\partial y} = \nu\frac{\partial^2 u}{\partial y^2} - \frac{\sigma B^2}{\rho(1+m^2)}(u + mw) - \frac{\nu}{k_1}u \quad (5)$$

$$\frac{\partial w}{\partial t} + u\frac{\partial w}{\partial x} + v\frac{\partial w}{\partial y} = \nu\frac{\partial^2 w}{\partial y^2} + \frac{\sigma B^2}{\rho(1+m^2)}(mu - w) - \frac{\nu}{k_1}w \quad (6)$$

$$\frac{\partial T}{\partial t} + u\frac{\partial T}{\partial x} + v\frac{\partial T}{\partial y} = \frac{K}{\rho c_p}\frac{\partial^2 T}{\partial y^2} - \frac{1}{\rho c_p}\frac{\partial q_r}{\partial y} + \frac{Q^*}{\rho c_p}(T - T_\infty) \quad (7)$$

$$\frac{\partial C}{\partial t} + u\frac{\partial C}{\partial x} + v\frac{\partial C}{\partial y} = D\frac{\partial^2 C}{\partial y^2} - k(C - C_\infty) - \frac{\partial}{\partial y}[V_T(C - C_\infty)] \quad (8)$$

Where T is the temperature inside the boundary layer, T_∞ is the ambient temperature, C is the fluid concentration, C_∞ is the ambient concentration, α is thermal diffusivity, ν is the kinematic viscosity, ρ is the density of the fluid, σ is the electrical conductivity, c_p is the specific heat at constant pressure, μ is the dynamic viscocity of the fluid, q_r is the radiative heat flux, K is the thermal conductivity of the medium, k_1 is the permeability of porous medium**,** D is the mass diffusivity, Q^* is the uniform volumetric heat absorption, k is the chemical reaction, V_T is the thermophoresis velocity, following Talbot et al. (1980) taken as $V_T = -\frac{k_t \nu}{T_{ref}}\frac{\partial T}{\partial y}$, where T_{ref} is some reference temperature, the value of $k_t\nu$ represents the thermophoretic diffusivity.

By using Rosseland approximation, the radiative heat flux is given by

$$q_r = -\frac{4\sigma^*}{3k^*}\frac{\partial T^4}{\partial y} \quad (9)$$

Where σ^* is the Stefen-Boltzman constant and k^* is the absorption coefficient.

T^4 may be linearly expanded in a Taylor's series about T_∞ to get

$$T^4 = T_\infty^4 + 4T_\infty^3(T - T_\infty) + 6T_\infty^2(T - T_\infty)^2 + \cdots, \quad (10)$$

and neglecting higher order terns beyond the first degree in $(T - T_\infty)$,

we obtain $T^4 \cong 4T_\infty^3\, T - 3T_\infty^4$ (11)

The boundary conditions of the problem are

$$u = U_w + N_1\nu\frac{\partial u}{\partial y},\quad v = -V_w(x,t),\quad w = N_1\nu\frac{\partial w}{\partial y},\quad -K\frac{\partial T}{\partial y} = h_f(T_f - T),\quad C = C_w(x,t) \qquad at \qquad y = 0, \quad (12)$$

$$u \to 0,\ w \to 0,\ T \to T_\infty,\ C \to C_\infty \qquad as \qquad y \to \infty \quad (13)$$

where $V_w(x,t) = (\nu U_w/x)^{1/2} fw$ represents the mass transfer at the surface with $V_w > 0$ for injection and $V_w < 0$ for suction, $N_1 = N_0(1 - ct)^{1/2}$ is the velocity slip factor which changes with time, N_0 is the initial value of the velocity slip factor (at $N_1 = 0$, the no-slip case is observed), h_f is the convective heat transfer coefficient and T_f is the convective fluid temperature.

The flow is induced by the stretching of the sheet which moves in its own plane with the surface velocity $U_w(x,t) = \frac{ax}{(1-ct)}$, where a (stretching rate) and c are the positive constants having dimension time^{-1} (with $ct < 1$, $c \geq 0$). It is noted that the stretching rate $\frac{a}{(1-ct)}$ increases with time since a > 0.

The convective fluid temperature of the sheet varies with square of distance x from the slot and time t in the form

$$T_f(x,t) = T_\infty + \frac{ax^2}{2\nu(1-ct)^{3/2}} \quad (14)$$

The surface concentration of the sheet varies with square of distance x from the slot and time t in the form

$$C_w(x,t) = C_\infty + \frac{ax^2}{2\nu(1-ct)^{3/2}} \quad (15)$$

where a is constant with $a \geq 0$. It should be noted that when t = 0 (initial condition), equations (5) – (8) describe the case of steady flow over a stretching sheet. The particular form of $U_w(x,t)$, $T_f(x,t)$ and $C_w(x,t)$ has been chosen in order to devise a similarity transformation which transforms the governing partial differential equations (5) – (8) into a set of highly nonlinear ordinary differential equations.

The stream function $\psi(x,y,t)$ is defined as:

$$u = \frac{\partial\psi}{\partial y} = \frac{ax}{(1-ct)}\, f'(\eta), \quad (16)$$

$$v = -\frac{\partial\psi}{\partial x} = -\left(\frac{\nu a}{1-ct}\right)^{1/2} f(\eta), \quad (17)$$

which automatically satisfies the continuity equation (4)

The governing partial differential equations (5) – (8) can be reduced to a set of ordinary differential equations on introducing the following similarity variables (Dulal Pal and Hiremath (2010)):

$$\psi(x,y,t) = \left(\frac{\nu a}{1-ct}\right)^{\frac{1}{2}} x f(\eta) \quad (18)$$

$$\eta = \sqrt{\frac{a}{\nu(1-ct)}}\,y \tag{19}$$
$$w = \frac{ax}{(1-ct)}\,g(\eta) \tag{20}$$
$$T(x,y,t) = T_\infty + \frac{ax^2}{2\nu(1-ct)^{3/2}}\theta(\eta), \quad \theta(\eta) = \frac{T-T_\infty}{T_f-T_\infty} \tag{21}$$
$$C(x,y,t) = C_\infty + \frac{ax^2}{2\nu(1-ct)^{3/2}}\phi(\eta), \quad \phi(\eta) = \frac{C-C_\infty}{C_w-C_\infty} \tag{22}$$
$$B^2 = B_0^2(1-ct)^{-1},\ Q^* = Q_0(1-ct)^{-1} \tag{23}$$

Substituting equations (18) – (23) into (5) – (8), we obtain
$$f''' + ff'' - f'^2 - A\left(f' + \frac{\eta}{2}f''\right) - \frac{M}{1+m^2}(f' + mg) - \lambda f' = 0 \tag{24}$$
$$g'' + fg' - f'g - A\left(g + \frac{\eta}{2}g'\right) + \frac{M}{1+m^2}(mf' - g) - \lambda g = 0 \tag{25}$$
$$\theta''\left(1 + \frac{4}{3}Nr\right) + Pr\left(f\theta' - 2f'\theta - \frac{A}{2}(3\theta + \eta\theta') + Q\theta\right) = 0 \tag{26}$$
$$\phi'' + Sc\left(f\phi' - 2f'\phi - \frac{A}{2}(3\phi + \eta\phi') - \tau(\theta'\phi' + \theta''\phi) - \gamma\phi\right) = 0 \tag{27}$$

The associated boundary conditions are
$$\eta = 0 \ : f = fw,\ f' = 1 + hf'',\ g = hg', \theta'(0) = -Bi(1-\theta(0)),\ \phi = 1 \tag{28}$$
$$\eta \to \infty :\ f' \to 0,\ g \to 0,\ \theta \to 0,\ \phi \to 0 \tag{29}$$
where the primes denote the differentiation with respect to η, $A = c/a$ is the unsteadiness parameter, $M = \sigma B_0^2/\rho a$ is the magnetic parameter, $\lambda = \nu(1-ct)/k_1 a$ is the porous parameter,$Pr = \rho c_p \nu/K$ is the Prandtl number, $Nr = 4\sigma^* T_\infty^3/Kk^*$ is the thermal radiation parameter, $Q = Q_0/a\rho c_p$ is the heat source/sink parameter, $Sc = \nu/D$ is the Schmidt number, $\gamma = k(1-ct)/a$ is the chemical reaction parameter, $\tau = -k_t(T_f - T_\infty)/T_{ref}$ is the thermophoretic parameter, $h = N_0(a\nu)^{1/2}$ is the velocity slip parameter and $Bi = \frac{h_f}{K}\sqrt{\frac{(1-ct)\nu}{a}}$ is the Biot number.

The physical quantities of engineering interest in this problem are the skin friction coefficient C_f, the local Nusselt number Nu_x and local Sherwood number Sh_x which are defined by
$C_{fx} = \frac{2\tau_{wx}}{\rho U_w^2}$, the skin friction coefficient in the x – direction
$C_{fz} = \frac{2\tau_{wz}}{\rho U_w^2}$, the skin friction coefficient in the z – direction
$$Nu_x = \frac{xq_w}{K(T_f - T_\infty)},\ Sh_x = \frac{xm_w}{D(C_w - C_\infty)} \tag{30}$$
where the wall shear stress τ_w, the surface heat flux q_w and mass flux m_w are given by
$$\tau_{wx} = \mu\left(\frac{\partial u}{\partial y}\right)_{y=0}, \qquad \tau_{wz} = \mu\left(\frac{\partial w}{\partial y}\right)_{y=0},$$
$$q_w = -K\left(\frac{\partial T}{\partial y}\right)_{y=0}, \qquad m_w = -D\left(\frac{\partial C}{\partial y}\right)_{y=0} \tag{31}$$

Using equation (31), the quantity (30) can be expressed as
$$\frac{1}{2}C_{fx}\sqrt{Re_x} = f''(0), \qquad \frac{1}{2}C_{fz}\sqrt{Re_x} = g'(0),$$
$$Nu_x/\sqrt{Re_x} = -\theta'(0), \qquad Sh_x/\sqrt{Re_x} = -\phi'(0), \tag{32}$$
where $\mu = \nu\rho$ is the dynamic viscosity of the fluid and Re_x is Reynolds number.

3. RESULTS AND DISCUSSION

In this investigation, we made an effort to analyze the effects of Hall currents, thermophoresis, thermal radiation and chemical reaction on the heat and mass transfer and flow of a viscous incompressible electrically conducting fluid past an unsteady porous stretching sheet embedded in a porous medium subject to a transverse magnetic field in the presence of heat source/sink with velocity slip and convective heat boundary condition. The equations (24) – (29) constitute a nonlinear coupled boundary value problem. It is difficult to obtain exact analytical solutions for this problem. Hence we employed the efficient finite difference method known as the Keller-box method. Computational results are obtained for a variety of physical parameters which are illustrated through graphs. In order to validate the accuracy of the numerical scheme applied we have compared our results, namely, wall temperature gradient of the present study with those of Chen (1998), Grubka and Bobba (1958), Aziz (2010) for different values of Prandlt number for a non permeable surface in the absence of diffusion equation, magnetic field, Hall currents, thermal radiation, heat source/sink and velocity slip for steady flow prescribing surface temperature ($M = m = \lambda = A = Nr = Q = \gamma = Sc = \tau = fw = h = Bi = 0$) and presented in Table 1 and are found to be in excellent agreement.

Table-1: Comparison of $-\theta'(0)$ for $M = m = \lambda = A = Nr = Q = \gamma = Sc = \tau = fw = h = Bi = 0$.

Pr	Chen (1998)	Gurbka and Bobba (1985)	Aziz (2010)	Present results
0.01	0.02942	0.0294	0.02948	0.02942
0.72	1.08853	1.0885	1.08855	1.08854
1.0	1.33334	1.3333	1.33333	1.33333
3.0	2.50972	2.5097	2.50972	2.50972
7.0	3.97150	-	3.97151	3.97151
10	4.79686	4.7969	4.79687	4.79686
100	15.7118	15.712	15.7120	15.7119

Figs. 2 – 5 present the influence of the magnetic field on the primary and secondary velocities, temperature and mass concentration. The presence of magnetic field decelerates the primary flow as a result of the resistive effect of the Lorentz force generated owing to the magnetic field which acts in the opposite direction to the fluid flow. Stronger magnetic fields result in further reduction in velocity and hence the thickness of the hydrodynamic boundary layers decreases. No secondary flow occurs in the absence of magnetic field and as the magnetic field strength increases a cross flow in the lateral direction is induced on account of the Hall currents. The secondary velocity is found to increase rapidly for increasing values of M in the vicinity of the boundary and attains its maximum and descends rapidly. For small values of M the velocity descends asymptotically to reach its free stream value. The temperature and the mass concentration are enhanced with increase in magnetic field strength and thus thermal boundary layer and mass concentration boundary layers are enlarged.

The effect of Hall parameter on the primary and secondary velocities, temperature and mass concentration is illustrated in Figs. 6 – 9. As mentioned above, the Lorentz force has a retarding effect on the primary velocity, this retardation is reduced with increase in the Hall parameter and hence the primary velocity is enhanced and consequently the hydrodynamic boundary layers become thicker. The secondary velocity increases as the Hall parameter m increases. The effect of Hall parameter on temperature and concentration is observed to be opposite to that of magnetic field. However, the variation in species concentration is small.

Figs. 10 – 13 reveal that primary and secondary velocities diminish with an increase in the unsteadiness parameter with a reduction in the thickness of the boundary layer. The temperature and concentration distributions also show a decreasing tendency with the unsteadiness parameter. The presence of porous medium causes a resistance to the fluid motion which leads to a reduction in both velocities (Figs. 14 and 15) and consequently the temperature and concentration rise. Fig. 16 shows that the temperature profiles increase with increasing porous parameter. Fig. 17 illustrates that the concentration increases in the solutal boundary layer with increasing values of porous parameter.

Fig. 18 presents the effect of Biot number on the thermal boundary layer. As Biot number increases convection becomes stronger resulting in higher surface temperature and the thermal effect penetrates deeper into the quiescent fluid. The thickness of corresponding thermal boundary layers increase. Fig. 19 illustrates that the temperature of higher Prandtl number fluids falls at a greater rate than the lower Prandtl number fluids. As Prandtl number is the ratio of the momentum diffusivity to thermal diffusivity, higher values of Pr correspond to diminishing of the thermal conductivity and hence the heat transfer from the heated plate takes place more rapidly for larger values of Prandtl number. Therefore, thermal boundary layer of higher Prandtl number fluids shrinks when compared to low Prandtl number fluids.

It is observed from Fig. 20 that increasing values of thermal radiation parameter produce thicker thermal boundary layers with a rise in temperature. The presence of $(1 + \frac{4}{3}\mathrm{Nr})/\mathrm{Pr}$ in the temperature equation (26) contributes for the rise in temperature for higher values of thermal radiation parameter. Fig. 21 depicts that the temperature is enhanced in the presence of heat source. The heat source releases energy in the thermal boundary layer resulting in the rise of temperature. On increasing $Q > 0$ (heat source) the temperature further rises. In the case of heat absorption $Q < 0$ (heat sink) the temperature drops with decreasing values of $Q < 0$ due to the absorption of energy in the thermal boundary layer.

From Fig. 22 it is evident that the concentration falls significantly when Schmidt number increases from 0.5 to 2. The influence of chemical reaction parameter (γ) on species concentration profile is plotted in Fig. 23. It is observed that an increase in the value of chemical reaction parameter reduces the concentration of species in the boundary layer owing to the fact that destructive chemical reaction reduces the solutal boundary layer and enhances the mass transfer. The influence of thermophoretic parameter on concentration is plotted in Fig. 24. It is observed that the effect of increasing the thermophoretic parameter is limited to decreasing the concentration. The concentration of the fluid steadily changes from higher value to the lower value and agreeing the free stream boundary condition as $\eta \to \infty$.

Figs. 25 – 28 depict the plots of velocities, temperature and concentration distribution for different values of suction. It is observed that the wall suction tends to reduce the thickness of the boundary layers. The temperature is observed to decrease with increasing suction parameter. Concentration is also observed to reduce for increasing values of suction. Figs. 29 and 30 display that the effect of velocity slip parameter h is to retard both the primary and secondary velocities as expected and consequently the temperature and concentration increase. It is evident from the Fig. 31 the temperature rises with increasing values of the slip parameter. The species concentration is also found to enhance for higher values of slip parameter (Fig. 32).

From Table 2 it is noted that the local skin friction coefficient $C_{fx}Re_x^{1/2}$ decreases for increasing values of magnetic parameter and shows an opposite trend for increasing values of Hall parameter. The skin friction coefficient $C_{fz}Re_z^{1/2}$ in the z-direction increases with increasing values of magnetic parameter, whereas the effect of Hall parameter is to enhance monotonically when m increases to 1.5 and reduces for values of m greater than 1.5. Salem and Aziz (2008) also noticed the same behaviour. The heat transfer coefficient (local Nusselt number $Nu_xRe_x^{-1/2}$) and the mass transfer coefficient (local Sherwood number $Sh_xRe_x^{-1/2}$) are observed to decrease for increasing values of magnetic parameter (M) while a totally reversal behaviour is noticed with an increase in the Hall parameter. The skin friction coefficient in both directions decrease with increasing values of unsteady parameter and an enhancement in the Nusselt number and Sherwood number is observed. The velocity slip parameter has a decreasing influence on skin friction coefficient in x and z – directions, heat and mass transfer coefficients. It is observed that higher Prandtl number fluids have higher values of Nusselt number. The effect of thermal radiation parameter (Nr) on the Nusselt number is opposite to that of the Prandtl number. Increasing values of Nr reduces Sherwood number. Increasing values of the heat source parameter ($Q > 0$) favour the heat and mass transfer rates whereas a reversal trend is found for increase in the sink parameter ($Q < 0$). As the Schmidt number increases, the Sherwood number enhances. The influence of chemical reaction parameter on Sherwood number is similar to that of the Schmidt number. Increasing values of thermophoresis parameter enhances the Sherwood number. The Nusselt number and Sherwood number are observed to increase with increasing values of suction. The effect of increasing suction on the Skin friction coefficient in the both directions is to decrease whereas the local Nusselt number and the local Sherwood number are enhanced. The velocity slip parameter increases the skin friction coefficient in the x-direction while it reduces in the z-direction. The local Nusselt number and the local Sherwood number are observed to decrease for increasing values of velocity slip parameter. The Biot number has a significant effect on the heat transfer coefficient producing an enhancement for increasing values of Biot number.

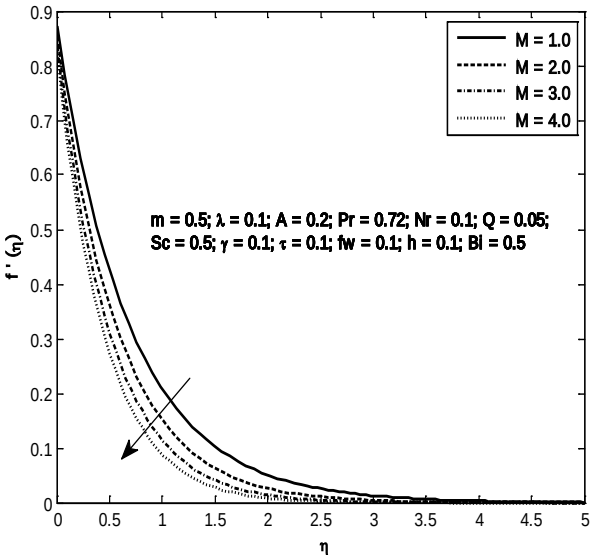

Fig. 2: Primary velocity profiles for different Values of M

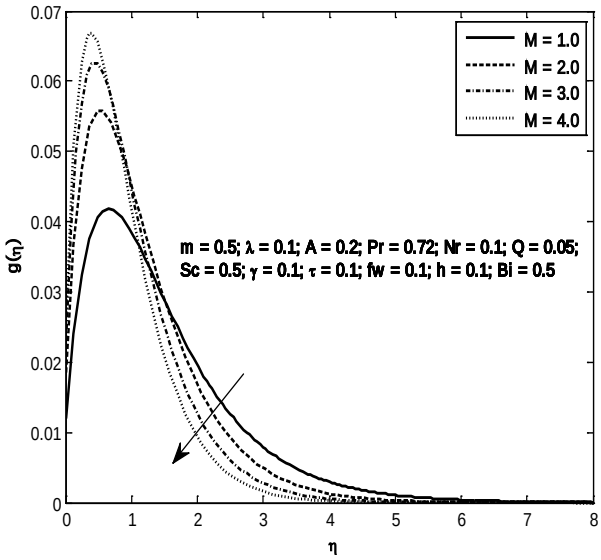

Fig. 3: Secondary velocity profiles for different Values of M

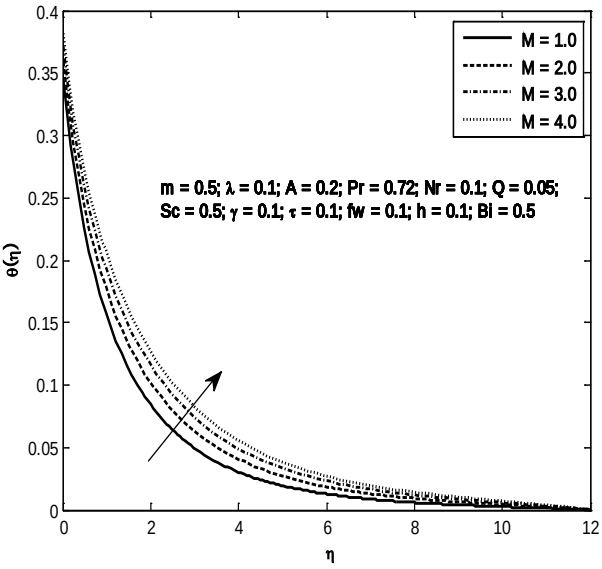

Fig. 4: Temperature profiles for different values of M

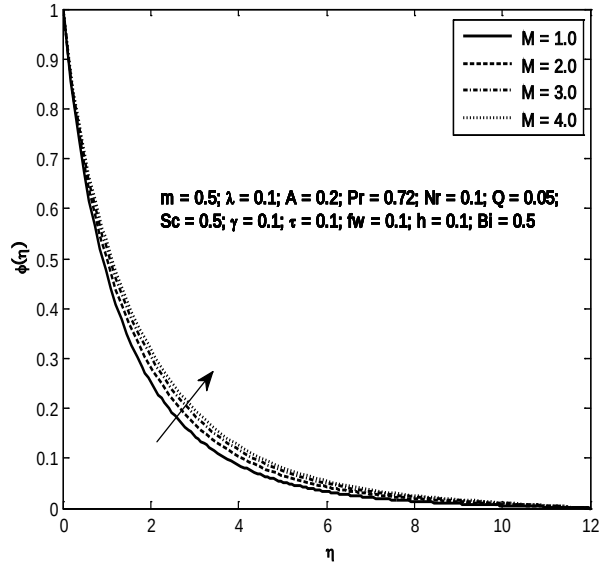

Fig. 5: Concentration profiles for different values of M

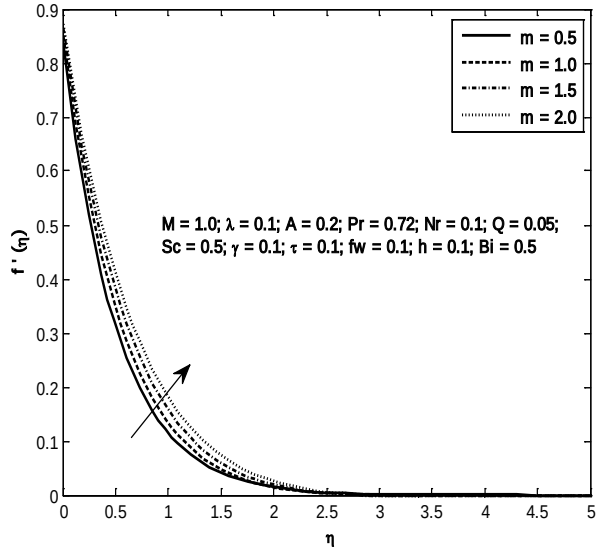

Fig. 6: Primary velocity profiles for different Values of m

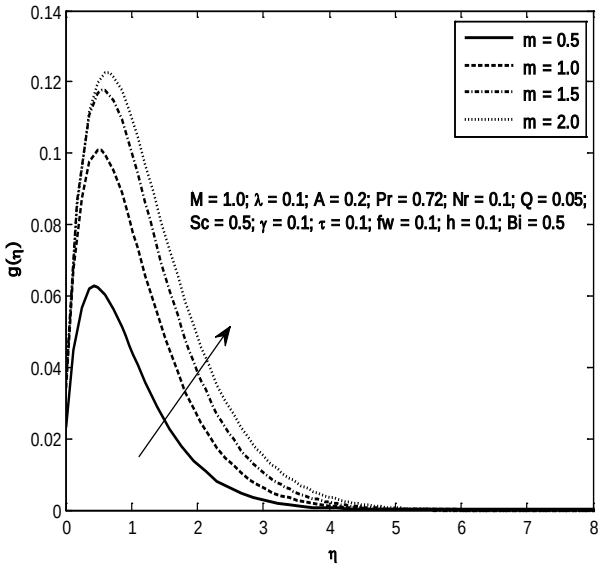

Fig. 7: Secondary velocity profiles for different Values of m

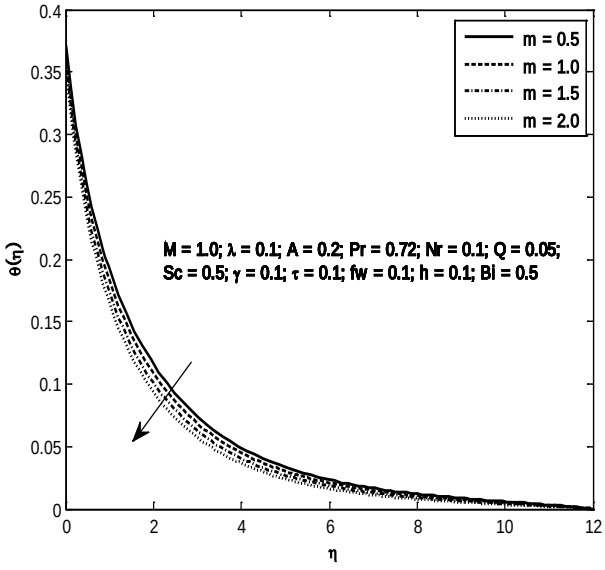

Fig. 8: Temperature profiles for different values of m

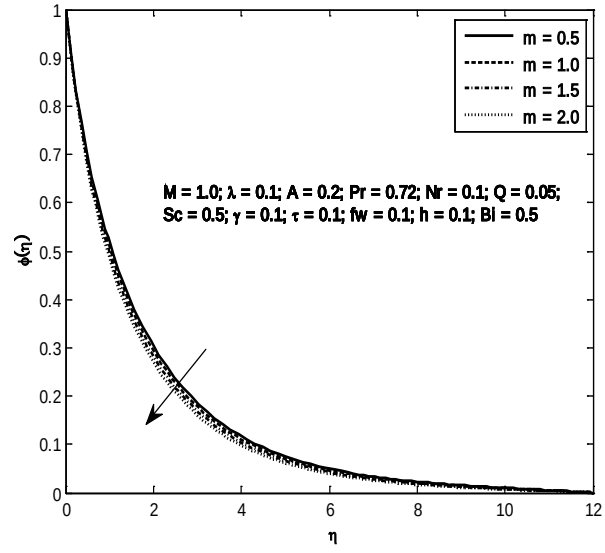

Fig. 9: Concentration profiles for different values of m

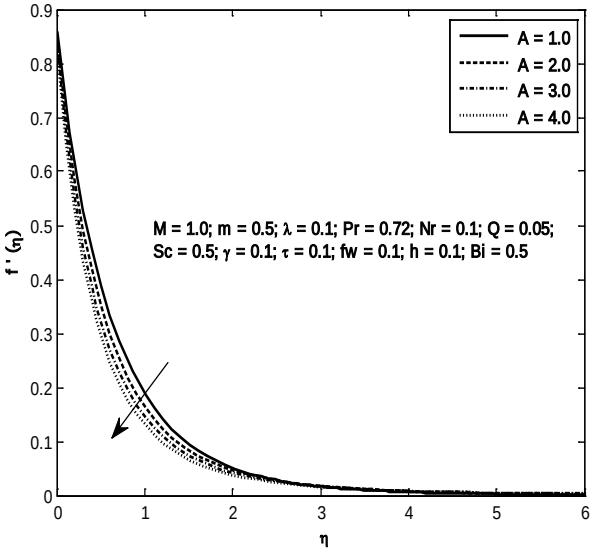

Fig. 10: Primary velocity profiles for different Values of A

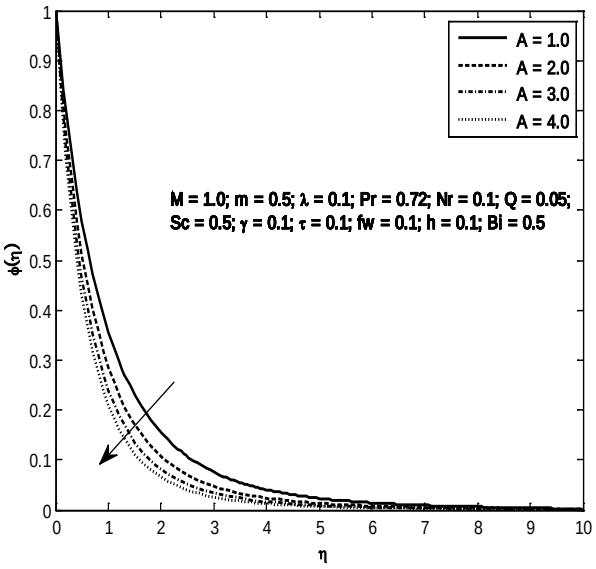

Fig. 13: Concentration profiles for different values of A

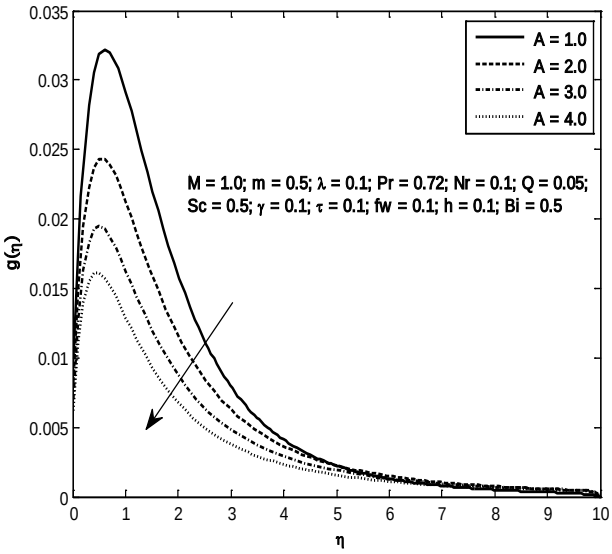

Fig. 11: Secondary velocity profiles for different Values of A

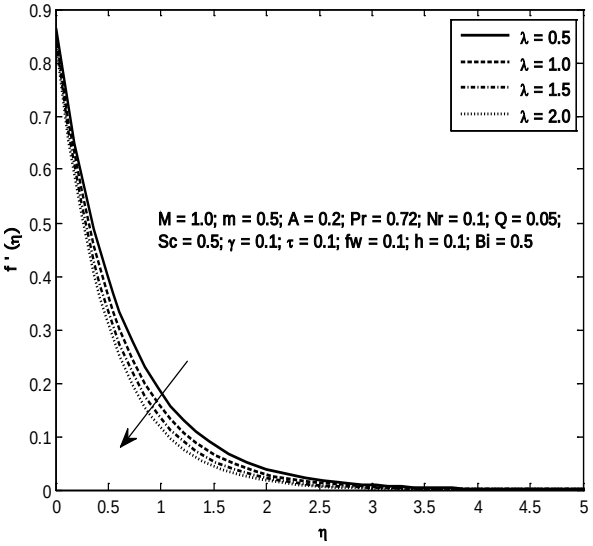

Fig. 14: Primary velocity profiles for different Values of λ

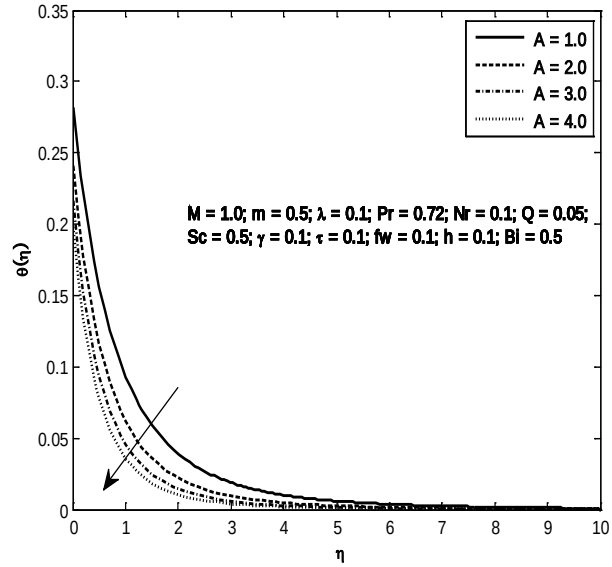

Fig. 12: Temperature profiles for different values of A

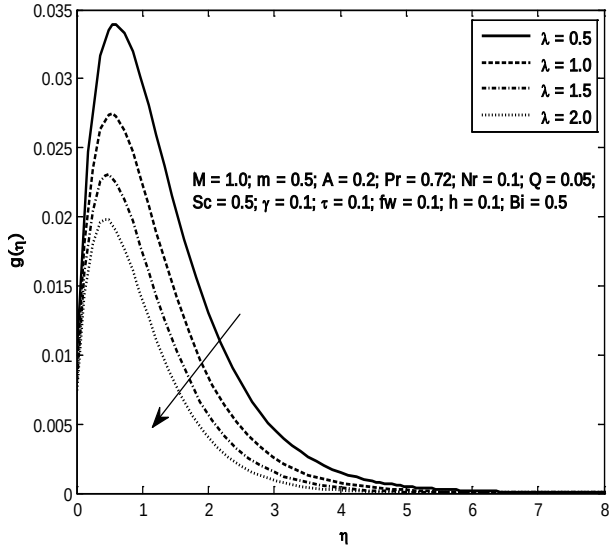

Fig. 15: Secondary velocity profiles for different Values of λ

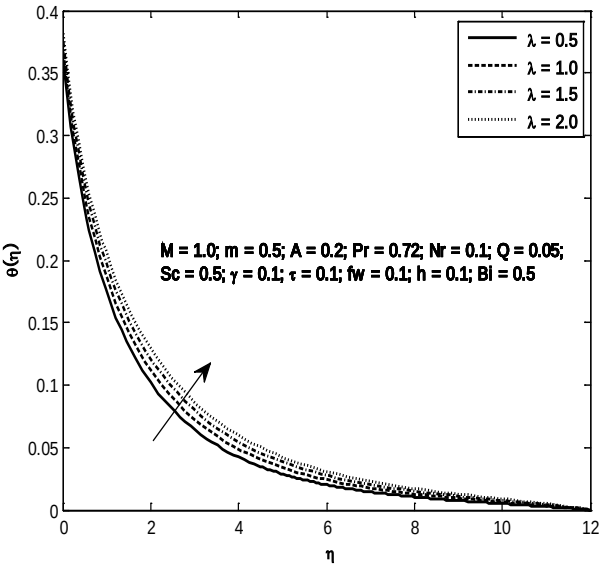

Fig. 16: Temperature profiles for different values of λ

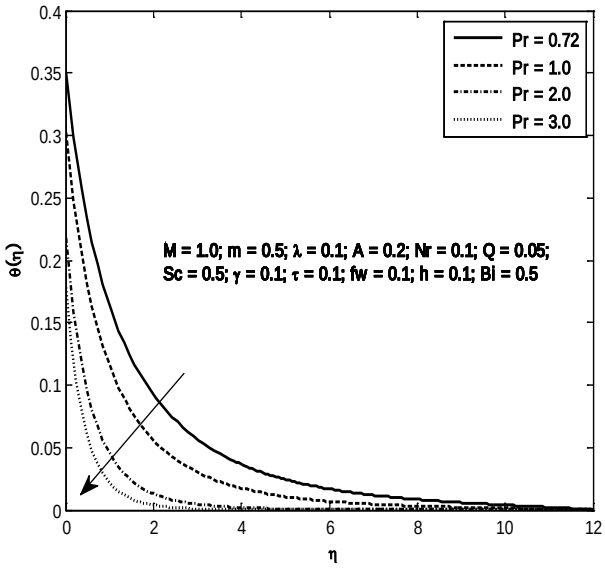

Fig. 19: Temperature profiles for different values of Pr

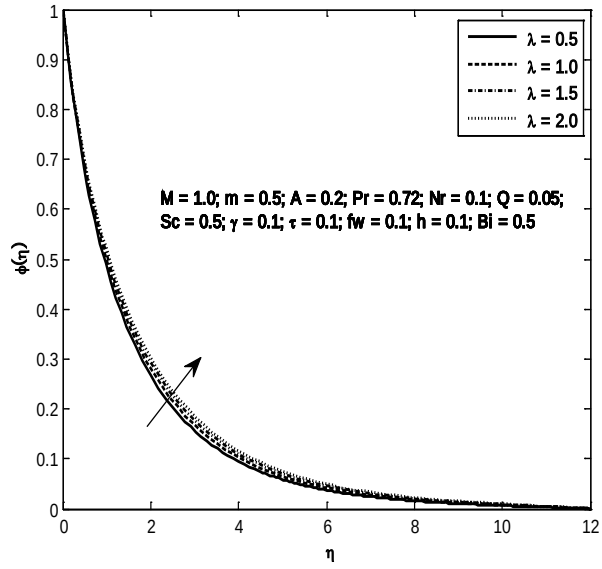

Fig. 17: Concentration profiles for different values of λ

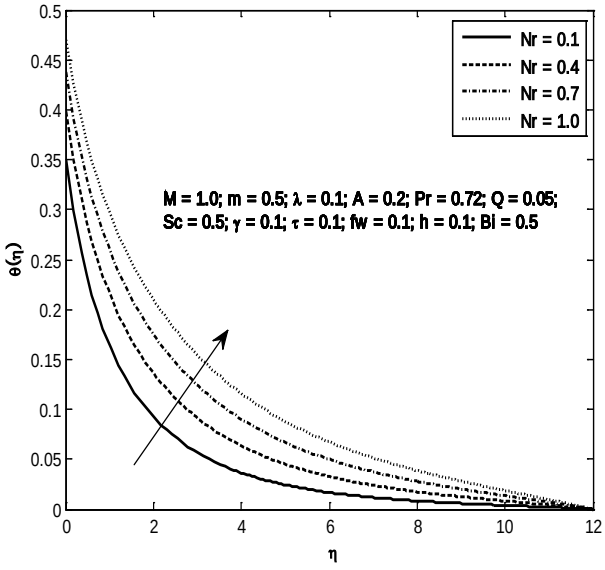

Fig. 20: Temperature profiles for different values of Nr

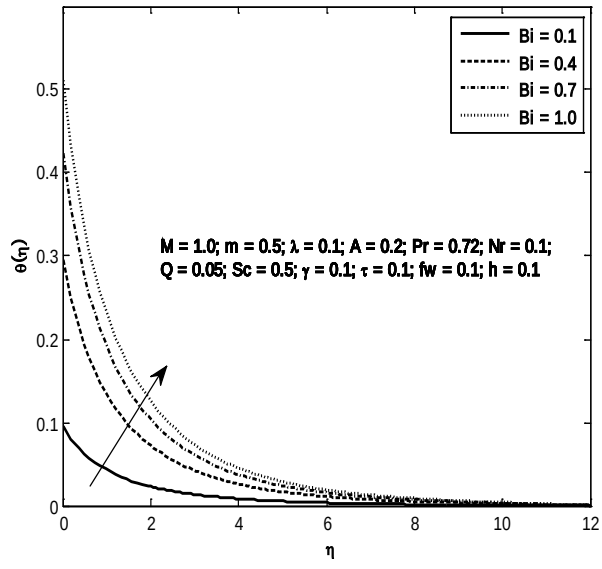

Fig. 18: Temperature profiles for different values of Bi

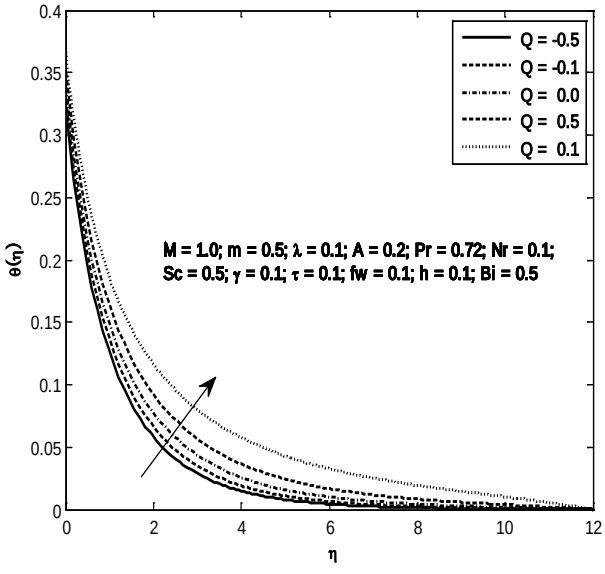

Fig. 21: Temperature profiles for different values of Q

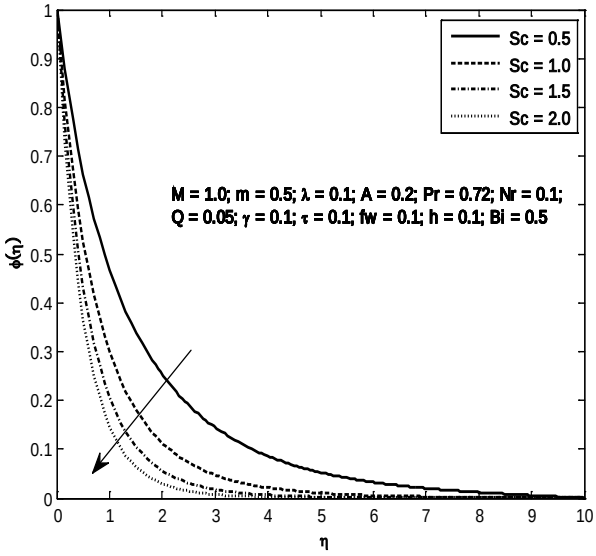

Fig. 22: Concentration profiles for different values of Sc

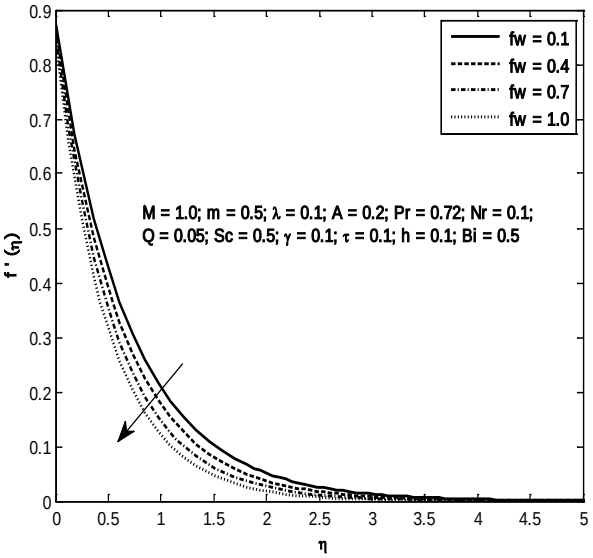

Fig. 25: Primary velocity profiles for different Values of fw

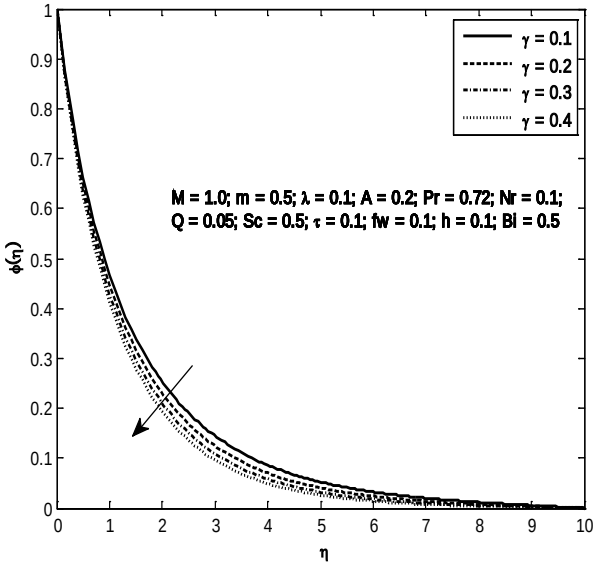

Fig. 23: Concentration profiles for different values of γ

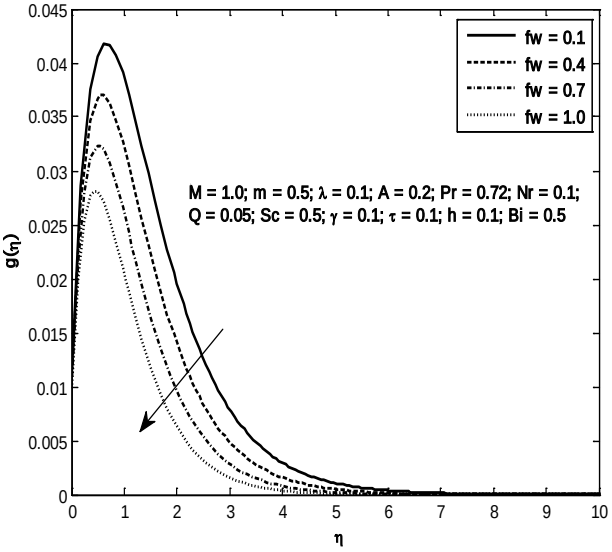

Fig. 26: Secondary velocity profiles for different Values of fw

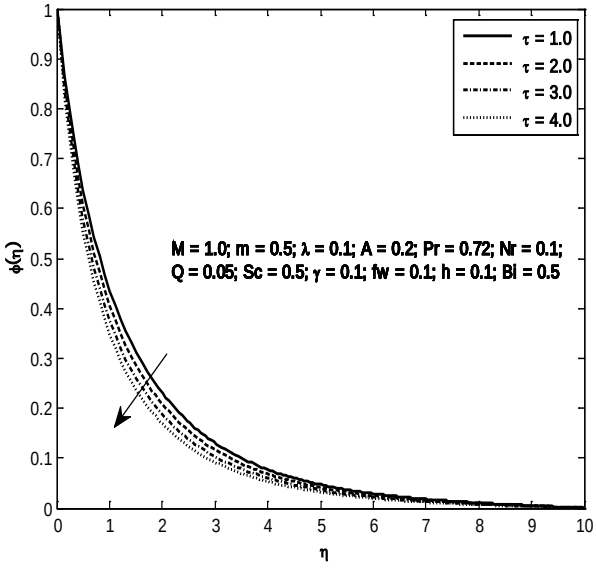

Fig. 24: Concentration profiles for different values of τ

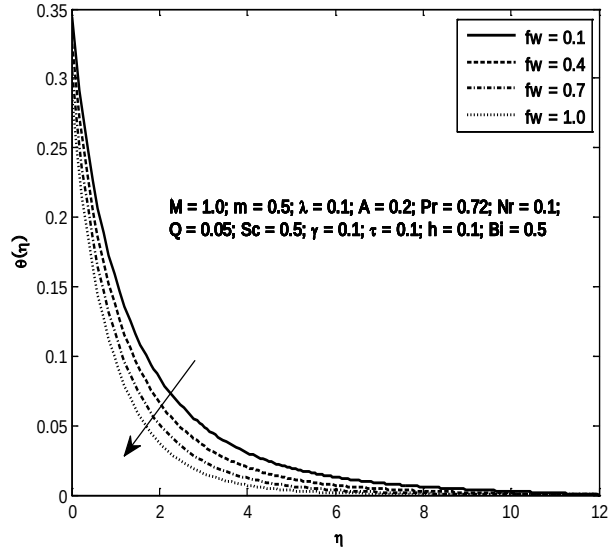

Fig. 27: Temperature profiles for different values of fw

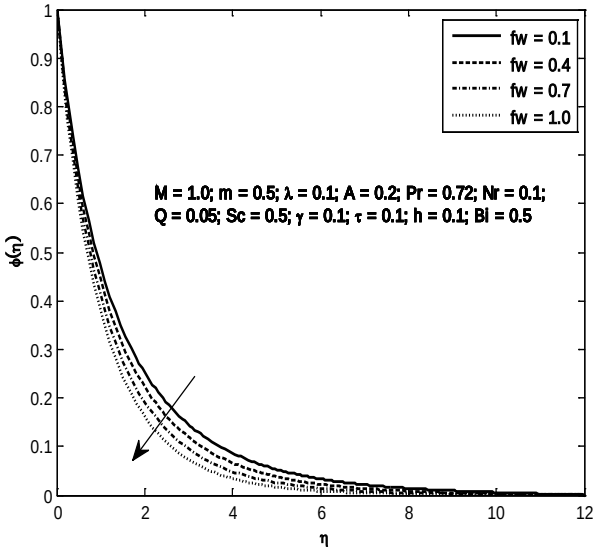

Fig. 28: Concentration profiles for different values of w

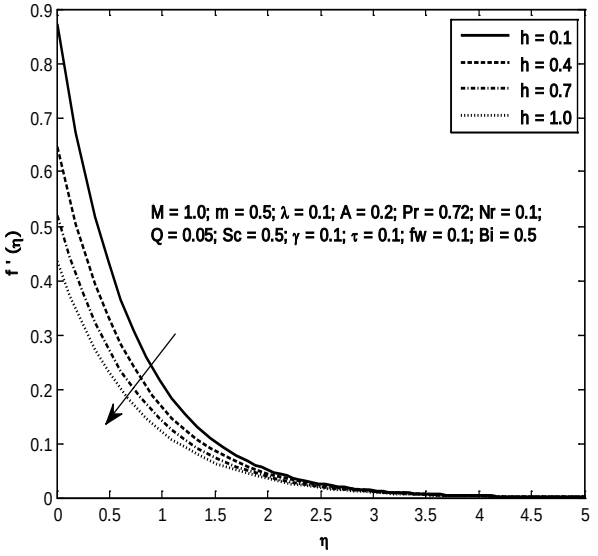

Fig. 29: Primary velocity profiles for different Values of h

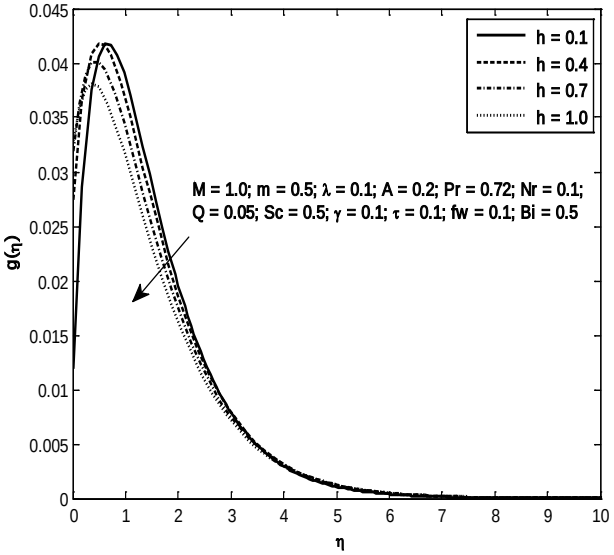

Fig. 30: Secondary velocity profiles for different Values of h

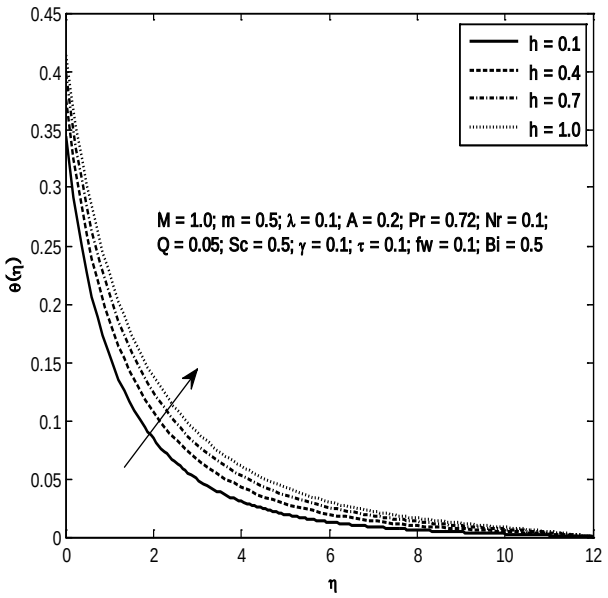

Fig. 31: Temperature profiles for different values of h

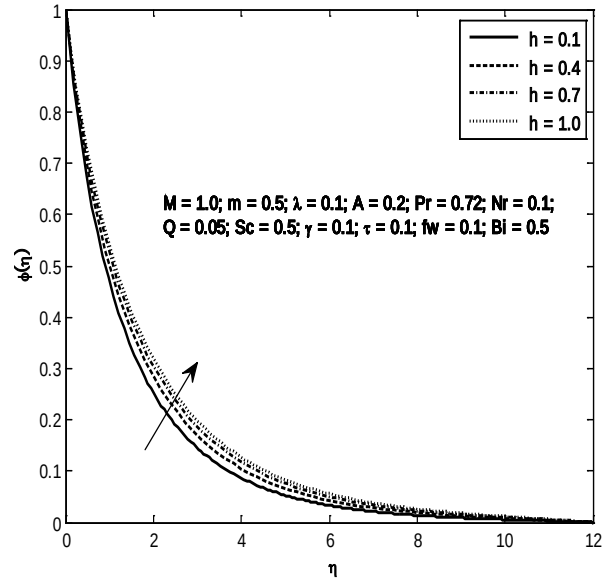

Fig. 32: Concentration profiles for different values of h

Table-2: Skin friction, Nusselt number and Sherwood number values for variation of different parameters

M	m	λ	A	Pr	Nr	Q	Sc	γ	τ	fw	h	Bi	$f''(0)$	$g'(0)$	$-\theta'(0)$	$-\phi'(0)$
1.0	0.5	0.1	0.2	0.72	0.1	0.05	0.5	0.1	0.1	0.1	0.1	0.5	-1.264241	0.119336	0.327964	0.891038
2.0													-1.467105	0.185284	0.320399	0.842532
3.0													-1.635682	0.230889	0.314233	0.806391
4.0													-1.781029	0.265597	0.309072	0.778115
1.0	0.5	0.1	0.2	0.72	0.1	0.05	0.5	0.1	0.1	0.1	0.1	0.5	-1.635682	0.230889	0.314054	0.805726
	1.0												-1.489627	0.341715	0.318066	0.829097
	1.5												-1.366128	0.366866	0.322012	0.853121
	2.0												-1.277822	0.356532	0.325199	0.873365
1.0	0.5	0.5	0.2	0.72	0.1	0.05	0.5	0.1	0.1	0.1	0.1	0.5	-1.363510	0.104729	0.320803	0.867348
		1.0											-1.474763	0.091541	0.316467	0.842722
		1.5											-1.574795	0.081764	0.312585	0.821762
		2.0											-1.665912	0.074161	0.309082	0.803643
1.0	0.5	0.1	1.0	0.72	0.1	0.05	0.5	0.1	0.1	0.1	0.1	0.5	-1.408287	0.099135	0.358930	1.173619
			2.0										-1.566642	0.082021	0.379277	1.431517
			3.0										-1.705245	0.070403	0.392007	1.644543
			4.0										-1.828476	0.061982	0.401107	1.831261
1.0	0.5	0.1	0.2	0.72	0.1	0.05	0.5	0.1	0.1	0.1	0.1	0.5	-1.264241	0.119336	0.324653	0.890432
				1.0									-1.264241	0.119336	0.348666	0.891592
				2.0									-1.264241	0.119336	0.391116	0.893871
				3.0									-1.264241	0.119336	0.410906	0.895081
1.0	0.5	0.1	0.2	0.72	0.0	0.05	0.5	0.1	0.1	0.1	0.1	0.5	-1.264241	0.119336	0.324653	0.890432
					0.4								-1.264241	0.119336	0.300630	0.889333
					0.7								-1.264241	0.119336	0.281249	0.888482
					1.0								-1.264241	0.119336	0.265140	0.887792
1.0	0.5	0.1	0.2	0.72	0.1	-0.2	0.5	0.1	0.1	0.1	0.1	0.5	-1.262779	0.136572	0.340123	0.891431
						-0.1							-1.262779	0.136572	0.335802	0.891242
						0.0							-1.262779	0.136572	0.330788	0.891031
						0.1							-1.262779	0.136572	0.324712	0.890791
						0.2							-1.262779	0.136572	0.316635	0.890500
1.0	0.5	0.1	0.2	0.72	0.1	0.05	0.5	0.1	0.1	0.1	0.1	0.5	-1.264241	0.119336	0.327884	0.890631
							1.0						-1.264241	0.119336	0.327884	1.380384
							1.5						-1.264241	0.119336	0.327884	1.773092
							2.0						-1.264241	0.119336	0.327884	2.112501
1.0	0.5	0.1	0.2	0.72	0.1	0.05	0.5	0.1	0.1	0.1	0.1	0.5	-1.264241	0.119336	0.327884	0.890631
								0.2					-1.264241	0.119336	0.327884	0.928797
								0.3					-1.264241	0.119336	0.327884	0.964089
								0.4					-1.264241	0.119336	0.327884	0.997157
1.0	0.5	0.1	0.2	0.72	0.1	0.05	0.5	0.1	1.0	0.1	0.1	0.5	-1.264241	0.119336	0.327884	1.003359
									2.0				-1.264241	0.119336	0.327884	1.130770
									3.0				-1.264241	0.119336	0.327884	1.260335
									4.0				-1.264241	0.119336	0.327884	1.391933
1.0	0.5	0.1	0.2	0.72	0.1	0.05	0.5	0.1	0.1	0.1	0.1	0.5	-1.264241	0.119336	0.327865	0.890557
										0.4			-1.382407	0.115093	0.337325	0.953862
										0.7			-1.508543	0.109384	0.347019	1.025550
										1.0			-1.641429	0.102609	0.356653	1.105822
1.0	0.5	0.1	0.2	0.72	0.1	0.05	0.5	0.1	0.1	0.1	0.1	0.5	-1.264241	0.119336	0.327865	0.890557
											0.4		-0.884522	0.068468	0.312253	0.794219
											0.7		-0.687008	0.045507	0.301282	0.736063
											1.0		-0.563935	0.032785	0.292919	0.696102
1.0	0.5	0.1	0.2	0.72	0.1	0.05	0.5	0.1	0.1	0.1	0.1	0.1	-1.264241	0.119336	0.090497	0.881571
												0.4	-1.264241	0.119336	0.281688	0.888808
												0.7	-1.264241	0.119336	0.403453	0.893421
												1.0	-1.264241	0.119336	0.487796	0.896618

4. CONCLUSIONS

The following conclusions are drawn:

- The Lorentz force has a retarding effect on the primary velocity and an opposite effect on the secondary velocity.
- Temperature enhances with higher values of porous parameter, Biot number, velocity slip parameter, heat source parameter, thermal radiation parameter and magnetic parameter while a reverse trend is observed with increase in the Hall parameter, unsteady parameter, suction parameter, heat sink parameter and Prandtl number.
- The species concentration increases for higher values of magnetic parameter, porous parameter and velocity slip parameter while a reversal effect is observed with Hall parameter, suction, thermophoretic parameter, Schmidt number and chemical reaction parameter.

- The skin friction coefficient in the x-direction increases with decrease in the magnetic parameter, unsteady and porous parameters and suction. The rate of heat transfer and mass transfer increase with increasing values of magnetic parameter and velocity slip parameter while a reverse effect is observed for increasing values of Hall parameter.
- The heat generation, thermal radiation favour rate of heat transfer.
- The thermophoretic parameter, Schmidt number, unsteady parameter and chemical reaction parameter have an enhancing influence on Sherwood number.

5. REFERENCES

1. Aziz M. A. E., Flow and heat transfer over an unsteady stretching surface with Hall effect, Meccanica, 45 (2010), 97 – 109.
2. Chen, C. H. Laminar mixed convection adjacent to vertical continuously stretching sheets, Heat and Mass Transfer, 33 (1998), 471 – 476.
3. Dulal Pal., Hall current and MHD effects on heat transfer over an unsteady stretching permeable surface with thermal radiation", Computers and Mathematics with Applications, 66 (2013), 1161 – 1180.
4. Eldahab E. M. A., Aziz M. A. E., Salem A. M., Jaber K. K., Hall current on MHD mixed convection flow from an inclined continuously stretching surface with blowing/suction and internal heat generation/absorption, Applied Mathematical Modelling, 31 (2007), 1829 – 1846
5. Goldsmith P. and May F.G., Diffusiophoresis and thermophoresis in water vapour systems, in Aerosol Science, Davies C.N. Davies (Ed.), Aerosol Science, Academic Press, London, (1966), 163 – 194.
6. Grubka L. J., Bobba K. M., Heat transfer characteristics of a continuous stretching surface with variable temperature, ASME J. Heat Transfer, 107 (1985), 248
7. Hales. J. M., Schwendiman L. C., Horst T. W., Aerosol transport in a naturally-convected boundary layer, Int. J. Heat Mass Transfer, 15 (1972), 1837 – 1849.
8. Sakiadis B. C., Boundary layer behavior on continuous solid surfaces: I. Boundary layer equations for two dimensional and axis symmetric flow, AIChE J., 7(26) (1961).
9. Salem A. M., Abd El – Aziz M., Effect of Hall currents and chemical reaction on hydromagnetic flow of a stretching vertical surface with internal heat generation/absorption, Applied Mathematical Modelling, 32 (2008), 1236 – 1254.
10. Seddeek M. A., Effects of radiation and variable viscosity on a MHD free convection flow past a semi-infinite flat plate with an aligned magnetic field in the case of unsteady flow, Int. J. Heat Mass Transfer, 45 (2002), 931 – 5.
11. Selim A., Hossain M. A., Rees D. A. S., The effect of surface mass transfer on mixed convection flow past a heated vertical flat plate permeable plate with thermophoresis, Int. J. of Thermal Sciences, 42 (2003), 973 – 982.
12. Talbot L., Cheng R. K., Schefer A. W., Wills D. R., Thermophoresis of particles in a heated boundary layer", Journal of Fluid Mechanics, 101(4) (1980), 737-758.
13. Vajravelu K., Convection Heat Transfer at a Stretching Sheet with Suction or Blowing, Journal of Mathematical Analysis and Applications, 188 (1994), 1002 – 1011.
14. Dulal Pal, Hiremath, P. S., Computational modeling of heat transfer over an unsteady stretching surface embedded in a porous medium, Meccanica, 45 (2010), 415 – 424.

Source of support: Nil, Conflict of interest: None Declared

Corresponding Author: Sarojamma G[3,*]
[1, 2, 3] Department of Applied Mathematics
Sri Padmavati Mahila Visvavidyalayam, Tirupati-517502, India.